Intermediates in membrane fusion and bilayer/nonbilayer phase transitions imaged by time-resolved cryo-transmission electron microscopy

D. P. Siegel, J. L. Burns, M. H. Chestnut, and Y. Talmon*
Procter & Gamble Company, Miami Valley Laboratories, Cincinnati, Ohio 45239-8707; and *Department of Chemical Engineering, Technion, Israel Institute of Technology, Haifa 32000, Israel

ABSTRACT Bilayer-to-nonbilayer phase transitions in phospholipids occur by means of poorly characterized intermediates. Many have proposed that membrane fusion can also occur by formation of these intermediates. Structures for such intermediates were proposed in a recent theory of these transition mechanisms. Using time-resolved cryo-transmission electron Microscopy (TRC-TEM), we have directly visualized the evolution of inverted phase microstructure in liposomal aggregates. We have identified one of the proposed intermediates, termed an interlamellar attachment (ILA), which has the structure and dimensions predicted by the theory. We show that ILAs are likely to be the structure corresponding to "lipidic particles" observed by freeze-fracture electron microscopy. ILAs appear to assemble the inverted cubic (I_{II}) phase by formation of an ILA lattice, as previously proposed. ILAs are also observed to mediate membrane fusion in the same systems, on the same time scale, and under nearly the same conditions in which membrane fusion was observed by fluorescence methods in earlier studies. These earlier studies indicated a linkage between a membrane fusion mechanism and I_{II} phase formation. Our micrographs suggest that the same intermediate structure mediates both of those processes.

INTRODUCTION

Transitions between phospholipid lamellar (L_α), inverted cubic (I_{II}), and inverted hexagonal (H_{II}) phases appear to occur by formation of discrete intermediate structures (1–5). Some of the proposed intermediates have also been invoked as mediators of the process of membrane fusion (1, 6–10), which has great biological significance (11–13). There is evidence that biomembrane lipid compositions are not far from $L_\alpha/I_{II}/H_{II}$ phase boundaries under physiological conditions (see citations in reference 3). Consequently, intermediates that form in these phase transitions might be relevant to membrane fusion and other dynamic processes in biomembranes. To understand the mechanism of bilayer/nonbilayer phase transitions and its relevance to membrane fusion, we must study the structure and formation kinetics of the intermediates.

A recently developed theory of the L_α/H_{II} transition mechanism (2–5) makes specific predictions concerning the structure and relative stability of the intermediates. According to this theory, all intermediates form between apposed bilayers in the L_α phase. Moreover, only two of the structures previously proposed for these intermediates should form at observable frequencies. One structure, the interlamellar attachment (ILA) (3, 4), is particularly interesting because it should mediate both membrane fusion and I_{II} phase formation at temperatures near T_H, the equilibrium L_α/H_{II} phase transition temperature. In support of this prediction, results of membrane fusion kinetics studies by Ellens, Bentz, and co-workers indicate that membrane fusion and I_{II} phase formation occur via the same structure (9, 10, 14).

Intermediate structures were first observed via freeze-fracture electron microscopy (FFEM) in systems near the L_α/H_{II} phase boundary and were called "lipidic particles" (15; see reference 1 for an excellent review). Several different structures were suggested for lipidic particles (16–21). Lipidic particles were proposed to be intermediates in $L_\alpha/I_{II}/H_{II}$ phase transitions (16, 22) and in membrane fusion (17, 22–24). However, to date it has not been possible to unambiguously establish the structure or structures corresponding to lipidic particle morphology in freeze-fracture electron micrographs.

Here, we use time-resolved cryo-transmission electron microscopy (TRC-TEM) (25–28) to image the evolution of microstructure in bilayer/nonbilayer transitions. This refinement of cryo-transmission electron microscopy permits the study of sample ultrastructure during different stages of a dynamic process (29). TRC-TEM has several advantages for the present study. First, samples are vitrified by rapid plunging into cryogen, which arrests the potentially labile morphology associated with these phase transitions (1, 2). Second, entire hydrated aggregates of liposomes can be imaged, as opposed to the single fracture planes through the specimen that are observed using freeze-fracture electron microscopy. Third, no stains or cryoprotectants are used, reducing the risk of artifacts.

Using this technique, we have visualized the predicted

0006-3495/89/07/161/09 $2.00

ILA intermediates and shown that ILAs appear to mediate both membrane fusion and the L_α/I_{II} phase transition. Our observations agree with both the predictions of the transition mechanism theory (2–5) and with the observed fusion kinetics of liposomal systems near bilayer/nonbilayer phase boundaries (9, 10, 14).

METHODS

Liposomes

Lyophilized phospholipids were purchased from Avanti Polar Lipids, Inc. (Birmingham, AL) and were used without further purification. Weighed amounts of phospholipid were hydrated in 100 mM $NaCl_2$, 20 mM glycine (pH 9.9), 0.1 mM EDTA (final lipid concentration of 10 or 20 mg/ml) for 1–2 h at 4°C with intermittent vortex mixing. The suspensions were subjected to three freeze-thaw cycles (dry ice, 40°C water bath) and then extruded through 0.1- or 0.2-μm pore-size filters (Nucleopore Corp., Pleasanton, CA) in a high-pressure extruder (Lipex Biomembranes, Vancouver, BC, Canada) at ~10°C. All the lipids used in this study were in the L_α phase under these conditions, except for egg phosphatidylethanolamine (EPE). EPE was hydrated in the same buffer but extruded at room temperature, where the L_α phase of this lipid is stable. Liposomes were stored on ice and observed the same day.

In TRC-TEM experiments, bilayer/nonbilayer transitions were induced in liposomal dispersions by rapidly changing the solution conditions to ones in which either H_{II} or I_{II} phase formation has been observed. In all the systems we studied, formation of nonbilayer phases can be triggered either by lowering the pH below ~8 or by adding Mg^{2+} at higher pH (9, 10, 30, 31). For example, DOPE is stable in the L_α phase when the pH is 9.5, where DOPE is anionic (10, 31). DOPE liposomes were made and stored under those conditions. At a pH below ~8, DOPE forms the H_{II} phase when the temperature is >10°C (32). Thus, we initiated nonbilayer phase formation in our DOPE liposomes by rapidly dropping the pH to 4.5 at 10–12°C. Similarly, EPE and DOPE-Me are stable in the L_α phase at pH 9.5, but form the H_{II} phase at lower pH or in the presence of Mg^{2+} at pH 9.5 (9, 10, 30, 31). The T_H for DOPE-Me at low pH is 66 ± 1°C, and is 60 ± 2°C in the presence of Mg^{2+} at pH 9.5 (9, 10). The corresponding T_H values for our samples of EPE were determined via DSC as described previously (10), and were found to be 35 ± 2° and 48 ± 2°C, respectively. The following buffers were used to achieve the required $[H^+]$ or $[Mg^{2+}]$ jumps: (*a*) 60 mM $MgCl_2$, 60 mM NaCl, 2 mM TES (pH 7.4); (*b*) 80 mM NaCl, 40 mM TES, 0.1 mM EDTA (pH 7.4); or (*c*) 100 mM NaCl, 50 mM sodium acetate, 0.1 mM EDTA (pH 4.5). These solutions were made roughly isoosmotic with the buffer in which liposomes were produced. Osmolalities were determined with a model 5500 vapor pressure osmometer (Wescor Inc., Logan, VT).

Time-resolved cryotransmission electron microscopy (TRC-TEM)

Our method is a refinement of earlier methods (25–28), and we describe it in detail elsewhere (29). It permits the study of sample ultrastructure during different stages of a dynamic process. Samples were prepared for vitrification in a temperature and humidity-controlled chamber (termed a CEVS) described previously (33). Phase transitions and membrane fusion were triggered in drops of liposomal dispersions on EM grids immediately before vitrification.

A 5-μl drop of liposomal dispersion was applied to a holey carbon film-covered EM grid in the CEVS. To trigger membrane fusion and bilayer/nonbilayer phase transitions, a 5-μl drop of an appropriate buffer solution was rapidly mixed with the first drop. Either immediately or after an interval of 3 s, most of the solution was blotted from the grid with filter paper to form a thin film specimen, which was immediately vitrified by plunging into liquid ethane at its freezing point. To prevent evaporation from the thin films before vitrification, the relative humidity was maintained at 85–95% at the indicated temperatures, except for studies around 10°C, where it was ~50%. After vitrification, the specimens were mounted in a cold stage (Gatan, Inc., Warrendale, PA) while under liquid nitrogen, transferred to a model H-500 TEM (Hitachi Ltd., Tokyo), and observed in the transmission mode at −165°C.

The time resolution in this study is on the order of seconds. The minimum time between sample mixing and fixation is 3 s, which is too long to permit time resolution of the steps in bilayer/nonbilayer phase transitions. Within 3 s, most of the sample transforms into large aggregates of liposomes and nonbilayer phase that are too electron-dense to yield detailed images. However, the mixing and blotting of the EM grid is inhomogeneous. This creates large disparities in the extent of microstructure evolution in different areas of a grid at a given time. As a consequence, it is often possible to image events with half-lives shorter than the sample preparation time scale. We are presently developing apparatus capable of producing a rapid temperature jump in a homogeneous, preblotted sample and vitrifying it within 0.1–0.2 s.

Freeze-fracture electron microscopy

DOPE-Me dispersions (10 mg/ml) were incubated in the presence of 30 mM Mg^{2+} at pH 9.5 for 20–30 min. An aliquot was placed between copper planchets (Balzers, Hudson, NH) and quenched immediately in liquid ethane at its freezing point. Samples were fractured at −120°C and replicated with Pt/C at an angle of 45° and C at an angle of 90° in a Balzers BAF400T. Replicas were cleaned with chloroform, and examined in a Hitachi 12A TEM.

THEORETICAL BACKGROUND

According to theory (2–5), there are two types of bilayer/nonbilayer phase transitions. We examined liposomal dispersions of phospholipids representative of both types. The first type, observed in dioleoylphosphatidylethanolamine (DOPE) (34) and egg phosphatidylethanolamine (EPE) (30), is a facile lamellar/inverted hexagonal (L_α/H_{II}) phase transition (3). In systems like DOPE and EPE, the transitions between the L_α and H_{II} phases should be rapid and comparatively nonhysteretic.

The second type of transition is typified by *N*-monomethylated dioleoylphosphatidylethanolamine (DOPE-Me), which exhibits very hysteretic L_α/H_{II} transitions (9, 10, 32, 35). This hysteresis involves the formation of "isotropic" or I_{II} phases at temperatures starting ~15–20° below T_H (9, 10). It has been proposed that this hysteresis is due to the formation of numerous intermediates known as ILAs, which rearrange into isotropic or I_{II} phases that are metastable over a broad temperature range (4, 5). The type of transition that occurs is determined by the tendency of a system to form ILAs.

ILAs are semi-toroidal (tire rim-shaped) bilayer attachments between flat bilayer sheets (Fig. 1 *A*). This structure is similar to one previously proposed for "lipidic particles" (1). We refer to the narrowest portion of an ILA in the plane between the two apposed bilayer sheets as the "waist." A lower limit to the outer diameter of the "waist" is the sum of the diameter of an H_{II} tube at T_H and the thickness of an L_α phase bilayer at the same temperature (5). Using data from (9, 10, 32), we find that this value is ~12 nm in DOPE-Me. ILAs should mediate bilayer membrane fusion because they form between two apposed bilayers and make them continuous (Fig. 1 *A*). When the two bilayers are the walls of vesicles, the aqueous contents of the vesicles become continuous through the pore created by the ILA, resulting in vesicle fusion.

The TRC-TEM experiments were performed to determine if ILA-like structures exist, in what subset of systems with bilayer/nonbilayer transitions ILAs form, and whether ILAs play the postulated role in bilayer/nonbilayer transitions and membrane fusion. We triggered the formation of nonbilayer structures in liposomal dispersions and then rapidly vitrified the specimens for examination with TRC-TEM. Triggering was accomplished by rapidly changing the solution conditions to ones in which either H_{II} or I_{II} phase formation has been observed. In all the systems we studied, formation of nonbilayer phases can be triggered either by a drop in pH below ~8 or by addition of Mg^{2+} at higher pH (10, 31). In each system, T_H is slightly different under these two different conditions. Presumably, T_H is different in the presence of Mg^{2+} and H^+ because these ions associate with the lipid head group in different ways. Thus, the ions reduce the charge and hydration of the head groups to different extents. Each of these has important effects on the relative stability of L_α and H_{II} phases (e.g., reference 37).

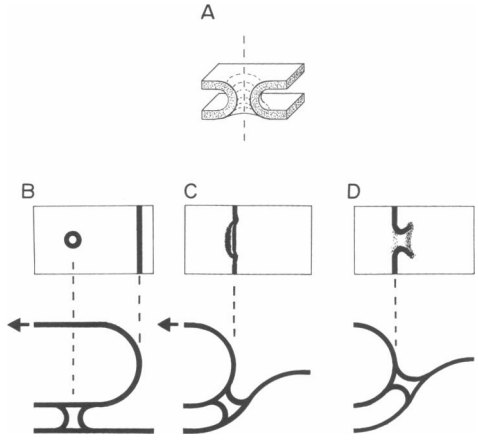

FIGURE 1 (*A*) Cross-section of an ILA (16). (*B*) ILA as it would appear in transmission microscopy when the bilayer stack is perpendicular to the electron beam (*top*) and parallel to the beam (*bottom*). A fold in one membrane is depicted. Flow in the aqueous film caused by capillary film thinning before fixation can move such a fold. In bilayer stacks lying in the sample plane, ILAs at these folds will be tilted almost into the sample plane, resulting in the morphology depicted in panels *C* and *D*.

RESULTS AND DISCUSSION

DOPE dispersions produced by high-pressure extrusion at pH 9.9 consist of uni- or oligolamellar liposomes ~0.1 μm in diameter (Fig. 2 *A*). Some of the liposomes are cylindrical or invaginated, rather than spherical. Similar morphology was also observed in dioleoylphosphatidylcholine (DOPC), EPE, and DOPE-Me dispersions produced in the same way (data not shown). The distortion of the liposomes may arise during the extrusion process, because liposomes produced by detergent dialysis are all nearly spherical (see below, and reference 38).

When the pH of DOPE dispersions is dropped to 4.5 at 11°C just before vitrification, the liposomes rapidly aggregate (Fig. 2 *B*), inclusions of H_{II} phase begin to form within aggregates (Fig. 2 *C*), and these domains grow at the expense of bilayer membrane until they dominate the sample. An aggregate in which the lipid is mostly in the H_{II} phase is shown in Fig. 2 *D* (DOPE acidified to pH 7.4 at 25°C). The H_{II} phase domains in Fig. 2 are distinguished by their optical density, and by the ~8 nm spacing of the dark lines within the domains. This spacing roughly matches the H_{II} tube width determined via x-ray diffraction at this temperature (32). Arrays of H_{II} tubes can occasionally be seen in cross-section (arrowheads in inset, Fig. 2 *C*).

We never observed H_{II} phase-like structures on the nonapposed surfaces of liposomes at pH 4.5 or 7.4. This indicates that the most rapid pathway to H_{II} phase formation is via intermediates that form between apposed membranes (2, 3). Qualitatively identical results were obtained in systems pH-jumped with a bilayer-permeating buffer (acetate, pH 4.5) or with an impermeant buffer (TES, pH 7.4). In acetate buffer, lipid molecules on both sides of the bilayers should be protonated nearly simultaneously (39, 40). Therefore, the lack of H_{II}-like morphology in nonapposed bilayers was not due to protonation of the lipids only on the exterior of the liposomes.

We could not further characterize the intermediate structures forming during L_α/H_{II} transitions in DOPE for two reasons. First, the pH jump immediately aggregates liposomes into clumps too electron dense to permit detailed visualization of the liposome–liposome interfaces. Second, the types of intermediates that form during facile L_α/H_{II} transitions may be too labile to be easily

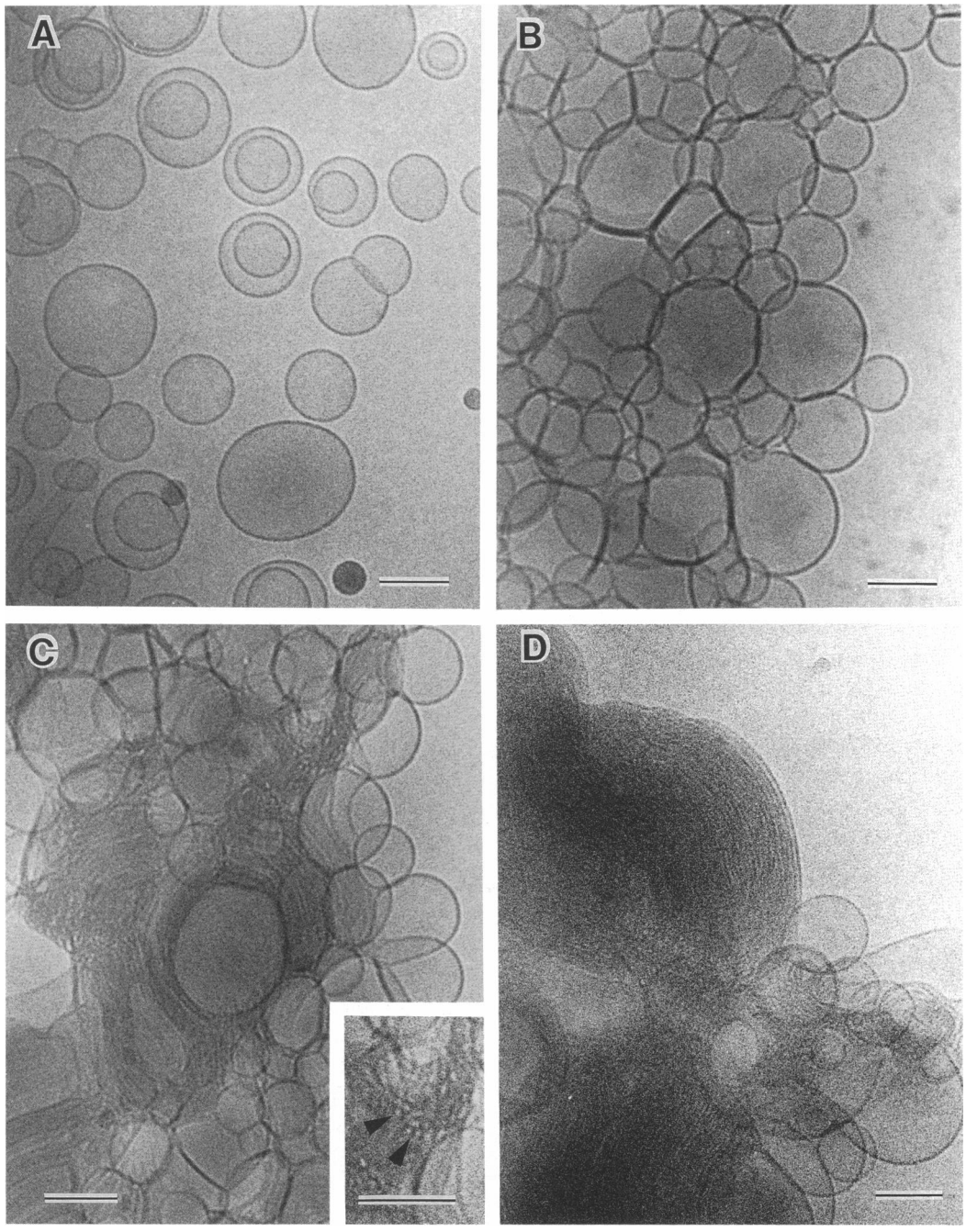

FIGURE 2 TRC-TEM images of DOPE liposomes. (*A*) DOPE liposomes at 25°C and pH 9.9 (where DOPE is stable in the L_α phase). (*B*) Aggregates of DOPE liposomes ~3 s after acidification to pH 4.5 with isoosmotic acetate buffer at 10.5°C. (*C*) H_{II} domains forming inside DOPE liposome aggregates. (*Inset*) Cross-sections of H_{II} tubes (*arrowheads*). (*D*) Large H_{II} domains ~5 s after acidification of DOPE with TES buffer (pH 7.4) at 25°C. Scale bar = 100 nm in all panels.

observable (1–3). We are currently developing methods for imaging intermediate structures in these systems.

We also examined DOPE-Me dispersions under conditions predicted to result in ILA formation (4, 5). The expected appearance of ILAs (5) within a bilayer stack viewed by TRC-TEM is indicated schematically in Fig. 1, *B–D*. In TRC-TEM, membranes produce the most contrast in an image when viewed edge-on to the beam. Thus, ILAs should appear as light-centered rings when the bilayers are perpendicular to the electron beam (Fig.

1 *B*, *top*) and as reversed parentheses when the bilayers are parallel to the beam (Fig. 1 *B*, *bottom*).

TRC-TEM images of DOPE-Me liposomes at pH 9.9, before addition of Mg^{2+}, were very similar to those of DOPE under the same conditions (data not shown). TRC-TEM images of DOPE-Me liposome suspensions vitrified ~6 s after addition of 30 mM Mg^{2+} at pH 9.5, and 50°C are displayed in Fig. 3, *A–C*. In Fig. 3 *A–C*, most of the liposomes have fused extensively, forming stacks of planar bilayers (this process is evident at the left and at the bottom of Fig. 3 *A*). Rings (arrowheads, Fig. 3 *B*) and reversed parentheses-figures (paired arrows, Fig. 3 *C*) corresponding to ILAs viewed in the orientations of Fig. 1 *B* (top and bottom, respectively) are clearly evident. The outer diameter of the rings and the narrowest width of the reversed parentheses figures are both ~15 nm. This value is consistent with the estimate of ILA "waist" diameter and with the tendency of ILAs to expand slightly immediately after formation (5). Note that the rings corresponding to top views of ILAs differ from the rings corresponding to cross-sections of H_{II} tubes (Fig. 2 *C*, *inset*) both in size and location. The rings corresponding to H_{II} tubes are much smaller than the rings corresponding to ILAs, and appear only in H_{II} domains, not in regions of apposed bilayers (Fig. 3 *A–C*).

The arrowheads in Fig. 3 *A* indicate what appear to be protrusions and elliptical features occurring at the edge of a membrane fold. We think that these features correspond to ILAs whose axes are tilted with respect to the plane of the sample, and which are tilted into that orientation by the motion of the edges of the membrane fold. This motion may be induced by thinning of the sample films by capillary suction of water into the periphery of the films; a phenomenon often observed in EM samples of this type (41). Film thinning induces radial flow in the film, and can result in motion of the folded edges of membranes as indicated in Fig. 1, *B–D*. ILAs at the margins of these folds would be tilted into different orientations with respect to the plane of the film. Because membranes viewed edge-on generate the most contrast in TRC-TEM images, these structures would yield the morphology depicted in Fig. 1, *C* and *D*. The predicted TRC-TEM images depicted in the upper parts of Fig. 1 *C* and *D*, are generated simply by drawing top views of the structures depicted in the bottom of each figure, shading the regions in which the bilayer would be exactly edge-on to the viewer, and erasing all other lines. These morphologies are very similar to the features indicated by arrowheads in Fig. 3 *A*. Moreover, the features indicated by arrowheads also have very nearly the same dimensions as the morphology thought to correspond to ILAs in other orientations (Figs. 3, *A–C*).

ILAs clearly mediate the fusion of the liposomes in DOPE-Me dispersions into large aggregates (Fig. 3 *A*, *bottom*). ILAs also appear on the same time scale as fusion of aggregated liposomes in this system under very similar conditions (9, 10). Many ILAs are observed via TRC-TEM within seconds after Mg^{2+} addition. Ellens et al. (9, 10) measured the rate of membrane fusion of DOPE-Me liposomes under conditions in which ILAs should form. Their results indicated that liposomes fused <1 s after aggregation (J. Bentz, personal communication), consistent with the ILA-mediated fusion apparent in Fig. 3 *A*.

Small numbers of ILAs were also observed at 36°C in this same system (data not shown). In contrast, samples prepared at 21°C showed no evidence of ILA formation (Fig. 3 *D*). The only structures visible in such micrographs are individual and aggregated liposomes. This is consistent with the results of Ellens et al. (10), who showed that isotropic ^{31}P-NMR resonances (which can arise from ILAs and ILA arrays; reference 5) first appear at 35°C in this system, and that the rate of membrane fusion (thought to be ILA-mediated) also begins to increase rapidly at 35°C.

No ILAs were observed in DOPE (Fig. 2). Systems like DOPE do not ordinarily form many ILAs or the isotropic or I_{II} phases that are proposed to form from ILAs (see references 4 and 5, and below).[1] Addition of certain types of surfactants may be able to induce isotropic phase formation in such systems (42). According to the kinetic theory (4, 5), these surfactants should greatly increase the ILA formation rate by increasing the spontaneous radius of curvature of the lipid-water interfaces of the system. If isotropic and I_{II} phases really are produced from ILAs, then these systems should exhibit ILA morphology. When we added the surfactant octyl glucoside to DOPE, we did observe ILA morphology. Fig. 3 *E* is a TRC-TEM image of a DOPE liposomal dispersion produced by dialysis of a DOPE/octyl glucoside mixture, obtained after the pH was reduced to 7.4 at 25°C. The octyl glucoside surfactant was incompletely removed by dialysis. The entire range of morphology is present simultaneously: L_α phase liposome aggregates, individual ILAs visible in a band of bilayers (small arrows), inclusions of isotropic/I_{II} phase (large arrows), and an H_{II} phase

[1]Shyamsunder et al. (36) induced an I_{II} phase in DOPE by temperature-cycling samples through T_H several hundred times. However, DOPE does not form an I_{II} phase spontaneously during incubations at $T < T_H$ or during a single heating through T_H (36). In theory (3–5), systems like DOPE form a very small number of ILAs during an L_α-to-H_{II} phase transition (too few to form I_{II} phases or to be observed easily with TRC-TEM). Once formed, however, ILAs can persist for long times at $T \leq T_H$. Each passage of the system through T_H forms a few ILAs. Exhaustive temperature-cycling through T_H eventually causes large numbers of ILAs to accumulate and assemble into isotropic or I_{II} phases.

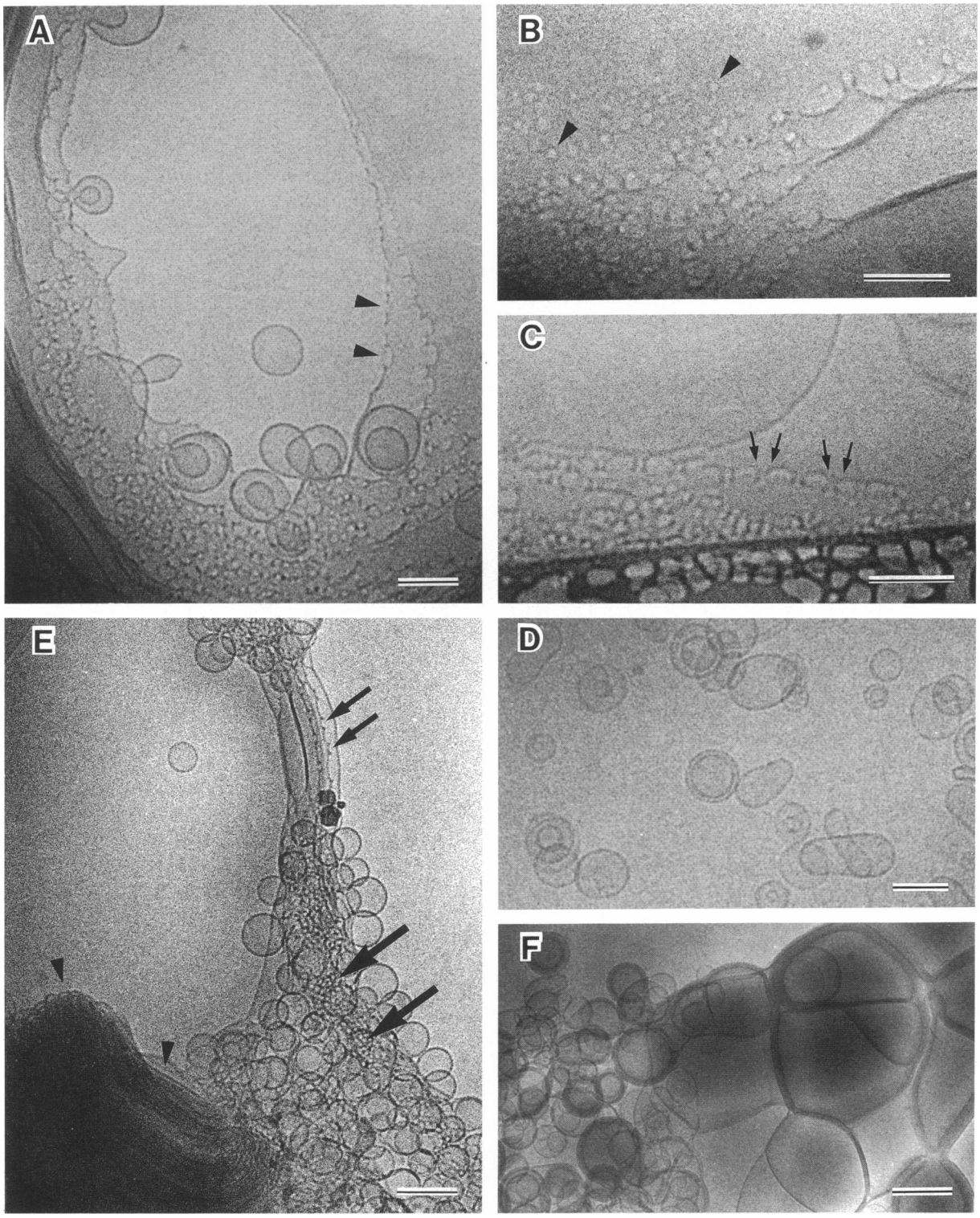

FIGURE 3 (*A*, *B* and *C*) TRC-TEM images of DOPE-Me suspensions at 50°C ~6 s after addition of isoosmotic Mg^{2+} buffer (30 mM, final concentration). ILAs are seen from the top ("rings," arrowheads in *B*) and side ("reversed parentheses," paired arrows in *C*), as described schematically in Fig. 1 *A*. ILAs at the edges of membrane folds, as depicted in Fig. 1, *C* and *D*, are also visible (arrowheads in *A*). The dark material at the bottom of *C* is the edge of a hole in the carbon film. (*D*) DOPE-Me suspension at 21°C ~6 s after addition of Mg^{2+} buffer. Only individual and aggregated liposomes, and no ILAs, are visible. (*E*) TRC-TEM image of DOPE/OG, acidified at 25°C. Note the individual ILAs (*small arrows;* cf Fig. 1 *C*) and aggregates of ILAs (*large arrows*), as well as an H_{II} phase domain (*arrowheads*). (*F*) EPE dispersion after acidification with isoosmotic TES buffer (pH 7.4) at 26°C. The liposomes have aggregated and formed multilamellar structures. No ILA-like morphology is visible. Scale bars = 100 nm in all panels except *F*, where it is 200 nm.

domain (arrowheads). The inclusions of isotropic or I_{II} phase are visible as superimposed rings ~15 nm in diameter: these probably represent ILAs forming between different pairs of bilayers within the multilayer stacks (see below).

The fact that ILA morphology is observed only in systems with hysteretic bilayer/nonbilayer transitions incubated at temperatures just below T_H is further emphasized by the absence of ILAs in EPE (Fig. 3 *F*). Like DOPE, EPE exhibits facile, comparatively nonhysteretic L_α/H_{II} phase transitions (30). EPE dispersions were incubated at low pH (Fig. 3 *F*) at 26°C, almost 10° below T_H. This is the same temperature relative to T_H at which DOPE-Me dispersions evolved numerous ILAs. We did not observe ILA morphology in EPE samples. The major structures visible in Fig. 3 *F* are optically-dense multilamellar structures forming in large liposomal aggregates. Similar results were obtained when EPE was incubated at high pH in the presence of Mg^{2+} at 38°C, 10°C below T_H in that buffer (data not shown).

ILAs were proposed (5) to be the structures responsible for "lipidic particle" morphology observed in FFEM. "Lipidic particles" have been observed to cluster into arrays correlated with the observation of the so-called "isotropic phase" and the I_{II} phase (1). We obtained FFEM images (Fig. 4 *A* and *B*) of the DOPE-Me system previously examined via TRC-TEM. A fracture plane traveling through one of the two membranes joined by an ILA would either shear the ILA off at the base or at the "waist." This probably results in the "pits and cusps," respectively, observed via FFEM (1). The density of lipidic particle images (Fig. 4 *A*) is similar to the density of ILA-like morphology in Fig. 3, *A–C*. In Fig. 4 *B*, the ILAs appear to have fractured through their "waists." A hint of the circular cross-section of the internal water pores is visible at the tips of the protrusions (arrowheads, Fig. 4 *B*). Hence, ILAs are probably the structures corresponding to "lipidic particle" morphology in FFEM.

It was also proposed (5) that the "isotropic phase" is actually a disordered array of ILAs, and that the first step in the L_α/I_{II} phase transition is the formation of an ordered lattice of ILAs from the "isotropic phase." The geometry and dimensions of this lattice have been predicted (5). The unit cell of this lattice is primitive tetragonal (Fig. 3 of reference 5). Between each pair of apposed bilayers, the ILAs should form a square lattice. The lattice constant can be estimated using the width of H_{II} tubes in the same system at the same temperature (extrapolated from higher temperature data). X-Ray diffraction data show that the H_{II} tube width in this system is 7.3 nm at T_H (10). Using the temperature coefficient of this width in DOPE-Me determined by Gruner et al. (32), the square lattice constant should be ~27.5 nm. If ILAs do mediate the L_α/I_{II} transition, then this ILA lattice ought to be observable with electron microscopy.

Our data indicate that ILAs form the "isotropic" phase and the proposed square lattice intermediate. In TRC-TEM, when ILAs are viewed along their axes, each ILA is visible as a ring, as illustrated in Fig. 1 *B*, *top*. In multilamellar stacks, ILAs form between each pair of

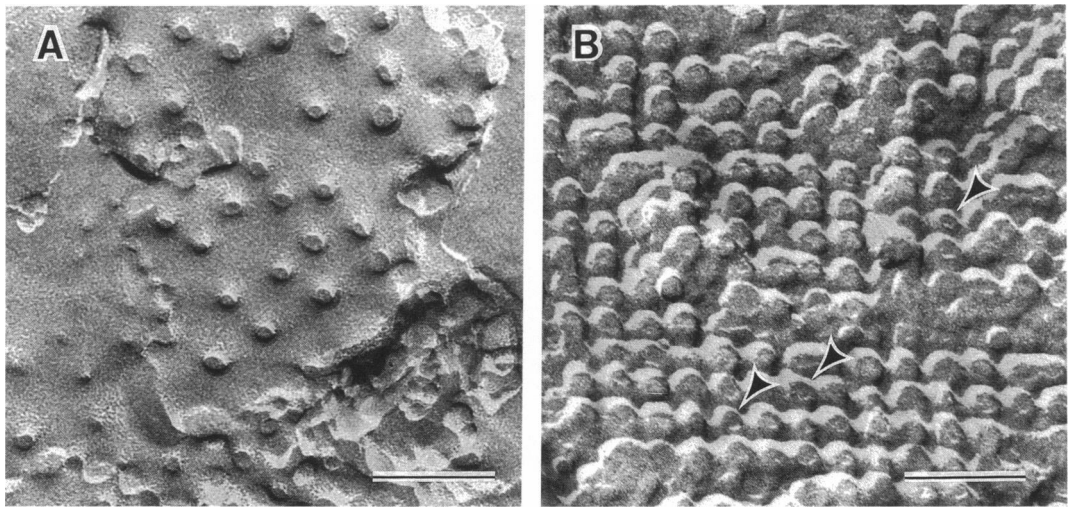

FIGURE 4 FFEM of DOPE-Me liposomes incubated with Mg^{2+} for 20–30 min at 50°C. The structures usually referred to as lipidic particles (1) seem to correspond to ILAs in TRC-TEM images (Fig. 3). (*A*) The ILAs are randomly arranged in the planes between apposed sheets of bilayer. (*B*) A square lattice of ILAs, with lattice constant ≈28 nm. Outlines of the water channels through the ILAs are discernible (*arrowheads*). Scale bars = 100 nm.

adjacent bilayers. This results in the images of superimposed rings visible at the bottom in Fig. 3 *A*. We think that such regions are equivalent to the region of FFEM replica bearing numerous but poorly ordered arrays of lipidic particles in Fig. 4 *A* (i.e., the "isotropic phase"). The well-ordered array of ILAs in Fig. 4 *B* appears to be the predicted square-lattice intermediate in I_{II} phase formation. The ILA axes are ~28 nm apart; in excellent agreement with the predicted value of 27.5 nm. Lattices of similar size and geometry were also observed previously (10).

CONCLUSION

The TRC-TEM images of DOPE liposome dispersions (Fig. 2) show no evidence of nonbilayer structure formation on the unapposed surfaces of liposomes. This is consistent with the prediction that the intermediates in this transition are interbilayer structures (2, 3). Figs. 1 and 3 show that structures with the geometry and dimensions proposed for ILAs do form during the anticipated type of bilayer/nonbilayer phase transitions. ILAs appear to be the lipidic particle structures previously observed via FFEM (1).

Fig. 3 shows that large numbers of ILAs appear in DOPE-Me/Mg^{2+} and DOPE/octyl glucoside, but not in DOPE and EPE. This is consistent with the ILA formation rate theory (4, 5), which predicts that numerous ILAs should form in systems with values of an interfacial curvature parameter like the values expected in DOPE-Me/Mg^{2+} and DOPE/octyl glucoside, but that very few ILAs will form in systems like DOPE and EPE. ILA morphology is observed in the systems that have been reported to form I_{II} phases (DOPE-Me) and in which isotropic and I_{II} phases appear to be forming (both DOPE-Me and DOPE/octyl glucoside; Fig. 3). This is consistent with the proposal that ILAs mediate the L_α/I_{II} phase transition (4, 5). ILAs appear to assemble the I_{II} phases via the intermediate ILA lattice predicted in reference 5.

Finally, ILAs appear to mediate membrane fusion of aggregated liposomes (Fig. 3). ILAs are observed by TRC-TEM within seconds after Mg^{2+} addition, which aggregates the liposomes in these concentrated dispersions within less than a second (as judged from the rate of turbidity development). Aqueous contents mixing assays of membrane fusion, done in the same lipid system under very similar conditions, also indicate that liposomes fuse within seconds or less after aggregation (9, 10). Thus, ILAs are probably the structures that mediate membrane fusion in nonbilayer phase-forming systems of this type, as previously proposed (4, 9, 10). Ellens et al. (9, 10) observed that a membrane fusion mechanism was associated with I_{II} phase formation, and speculated that the processes had an intermediate in common. Our micrographs are direct evidence that the same intermediate structure does mediate both of those processes.

The authors are grateful to Dr. John R. Silvius for a helpful discussion of liposome morphology, Dr. Joe Bentz for helpful discussions of fusion kinetics in these systems, Dr. Ronald R. Warner and Dr. Anne Walter for comments on the manuscript, and to Mr. James L. Banschbach for expect technical assistance.

Received for publication 30 January 1989 and in final form 27 March 1989.

Note added in proof: Frederik, P. M., et al. (1989. *Biochim. Biophys. Acta.* 979:275–278) recently published a similar study of intermediate structures in different nonbilayer-phase phospholipid systems. Their results appear to be roughly consistent with ours.

REFERENCES

1. Verkleij, A. J. 1984. Lipidic intramembranous particles. *Biochim. Biophys. Acta.* 779:43–63.
2. Siegel, D. P. 1984. Inverted micellar structures in bilayer membranes. *Biophys. J.* 45:399–420.
3. Siegel, D. P. 1986. Inverted micellar intermediates and the transitions between lamellar, cubic and inverted hexagonal lipid phases. I. Mechanism of the $L_\alpha <-> H_{II}$ phase transition. *Biophys. J.* 49:1155–1150.
4. Siegel, D. P. 1986. Inverted micellar intermediates and the transitions between lamellar, cubic and inverted hexagonal lipid phases. II. Implications for membrane-membrane interactions and membrane fusion. *Biophys. J.* 49:1171–1183.
5. Siegel, D. P. 1986. Inverted micellar intermediates and the transitions between lamellar, cubic, and inverted hexagonal amphiphile phases. III. Isotropic and inverted cubic state formation via intermediates in transitions between L_α and H_{II} phases. *Chem. Phys. Lipids.* 42:279–301.
6. Rilfors, L., G. Lindblom, A. Wieslander, and A. Christiansson. 1984. Lipid bilayer stability in biological membranes. *In* Biomembranes. Vol. 12. M. Kates and L. A. Manson, editors. Plenum Publishing Corp., New York. 205–245.
7. Gruner, S. M., P. R. Cullis, M. J. Hope, and C. P. S. Tilcock. 1985. Lipid polymorphism: the molecular basis of nonbilayer phases. *Annu. Rev. Biophys. Biophys. Chem.* 14:211–238.
8. Cullis, P. R., M. J. Hope, and C. P. S. Tilcock. 1986. Lipid polymorphism and the roles of lipids in membranes. *Chem. Phys. Lipids.* 40:127–144.
9. Ellens, H., J. Bentz, and F. C. Szoka. 1986. Fusion of phosphatidylethanolamine liposomes and the mechanism of the $L_\alpha - H_{II}$ phase transition. *Biochemistry.* 25:4141–4147.
10. Ellens, H., D. P. Siegel, D. Alford, P. Yeagle, L. Boni, L. Lis, P. J. Quinn, and J. Bentz. 1989. Membrane fusion and inverted phases. *Biochemistry.* 28:3692–3703.
11. Poste, G., and G. L. Nicolson, editors. 1985. Membrane Fusion. Vol. 5. North-Holland Publishing Co., Amsterdam.
12. Düzgüneş, N. 1985. Membrane fusion. *In* Subcellular Biochemistry. Vol. 11. D. B. Roodyn, editor. Plenum Publishing Corp., New York. 195–286.

13. Sowers, A. E., editor. 1987. Cell Fusion. Plenum Publishing Co., New York.

14. Siegel, D. P., J. L. Banschbach, D. Alford, H. Ellens, L. J. Lis, P. J. Quinn, P. L. Yeagle, and J. Bentz. 1989. Physiological levels of diacylglycerols in phospholipid membranes induce membrane fusion and stabilize inverted phases. *Biochemistry.* 28:3703–3709.

15. Verkleij, A. J., C. Mombers, J. Lenissen-Bijvelt, and P. H. J. Th. Ververgaert. 1979. Lipidic intramembranous particles. *Nature (Lond.).* 279:162–163.

16. Hui, S. W., T. P. Stewart, and L. T. Boni. 1983. The nature of lipidic particles and their roles in polymorphic transitions. *Chem. Phys. Lipids.* 33:113–126.

17. Rand, R. P., T. S. Reese, and R. G. Miller. 1981. Phospholipid bilayer deformations associated with interbilayer contact and fusion. *Nature (Lond.).* 293:237–238.

18. Miller, R. G. 1980. Do "lipidic particles" represent intermembrane attachment sites? *Nature (Lond.).* 287:166–167.

19. Hui, S. W., and T. P. Stewart. 1981. "Lipidic particles" are intermembrane attachment sites. *Nature (Lond.).* 290:427.

20. Sen, A., W. Patrick Williams, A. P. R. Brain, M. J. Dickens, and P. J. Quinn. 1981. Formation of inverted micelles in dispersions of mixed galactolipids. *Nature (Lond.).* 293:488–490.

21. Hui, S. W., and L. T. Boni. 1982. Lipidic particles and cubic phase lipids. *Nature (Lond.).* 296:175.

22. Verkleij, A. J., C. J. A. Van Echteld, W. J. Gerritsen, P. R. Cullis, and B. De Kruijff. 1980. The lipidic particle as an intermediate structure in membrane fusion processes and bilayer to hexagonal (H_{II}) transitions. *Biochim. Biophys. Acta.* 600:620–624.

23. Cullis, P. R., and M. J. Hope. 1978. Effects of fusogenic agent on membrane structure of erythrocyte ghosts and the mechanism of membrane fusion. *Nature (Lond.).* 271:672–674.

24. Verkleij, A. J., C. Mombers, W. J. Gerritsen, L. Leunissen-Bijvelt, and P. R. Cullis. 1978. Fusion of phospholipid vesicles in association with the appearance of lipidic particles as visualized by freeze fracturing. *Biochim. Biophys. Acta.* 555:358–361.

25. Talmon, Y. 1986. Imaging surfactant dispersions by electron microscopy of vitrified specimens. *Colloids Surf.* 19:237–248.

26. Miller, D. D., J. R. Bellare, D. F. Evans, Y. Talmon, and B. W. Ninham. 1987. Meaning and structure of amphiphilic phases: inferences from video-enhanced microscopy and cryotransmission electron microscopy. *J. Phys. Chem.* 91:674–685.

27. Adrian, M., J. Dubochet, J. Lepault, and A. W. McDowall. 1984. Cryoelectron microscopy of viruses. *Nature (Lond.).* 308:32–36.

28. Dubochet, J., M. Adrian, J. Lepault, and A. W. McDowall. 1985. Cryoelectron microscopy of vitrified biological specimens. *Trends Biochem. Sci.* 10:143–146.

29. Talmon, Y., J. L. Burns, M. H. Chestnut, and D. P. Siegel. 1989. Time-resolved cryo-transmission electron microscopy. *J. Electron Microsc. Tech.* In press.

30. Cullis, P. R., and B. De Kruijff. 1978. The polymorphic phase behavior of phosphatidylethanolamines of natural and synthetic origin. *Biochim. Biophys. Acta.* 513:31–42.

31. Ellens, H., J. Bentz, and F. C. Szoka. 1986. Destabilization of phosphatidylethanolamine liposomes at the hexagonal phase transition temperature. *Biochemistry.* 25:285–294.

32. Gruner, S. M., M. W. Tate, G. L. Kirk, P. T. C. So, D. C. Turner, D. T. Keane, C. P. S. Tilcock, and P. R. Cullis. 1988. X-Ray diffraction study of the polymorphic behavior of *N*-mono-methylated dioleoylphosphatidylethanolamine. *Biochemistry.* 27:2853–2866.

33. Bellare, J. R., H. T. Davis, L. E. Scriven, and Y. Talmon. 1988. Controlled environment vitrification system: an improved sample preparation technique. *J. Electron Microsc. Tech.* 10:87–111.

34. Tilcock, C. P. S., and P. R. Cullis, 1982. The polymorphic phase behavior and miscibility properties of synthetic phosphatidylethanolamines. *Biochim. Biophys. Acta.* 684:212–218.

35. Gagné, J., L. Stamatatos, T. Diacovo, S. W. Hui, P. L. Yeagle, and J. R. Silvius. 1985. Physical properties and surface interactions of bilayer membranes containing *N*-methylated phosphatidylethanolamines. *Biochemistry.* 24:4400–4408.

36. Shyamsunder, E., S. M. Gruner, M. W. Tate, D. C. Turner, P. T. C. So, and C. P. S. Tilcock. 1988. Observation of inverted cubic phase in hydrated dioleoylphosphatidylethanolamine membranes. *Biochemistry.* 27:2332–2336.

37. Kirk, G. L., S. M. Gruner, and D. L. Stein. 1984. A thermodynamic model of the lamellar to inverse hexagonal phase transition of membrane-water systems. *Biochemistry.* 23:1093–1102.

38. Lepault, J., F. Pattus, and N. Martin. 1985. Cryo-electron microscopy of artificial biological membranes. *Biochim. Biophys. Acta.* 820:315–318.

39. Barbet, J., P. Machy, A. Truneh, and L. D. Leserman. 1984. Weak acid-induced release of liposome-encapsulated carboxyfluorescein. *Biochim. Biophys. Acta.* 772:347–356.

40. Bentz, J., H. Ellens, and F. C. Szoka. 1987. Destabilization of phosphatidylethanolamine-containing liposomes: hexagonal phase and asymmetric membranes. *Biochemistry.* 26:2105–2116.

41. Dubochet, J., M. Adrian, J. J. Chang, J. C. Homo, J. Lepault, A. W. McDowall, and P. Schultz. 1988. Cryo-electron microscopy of vitrified specimens. *Q. Rev. Biophys.* 21:129–228.

42. Wieslander, A., L. Rilfors, and G. Lindblom. 1986. Metabolic changes of membrane lipid composition in *Acholeplasma laidlawii* by hydrocarbons, alcohols, and detergents: Arguments for effects on lipid packing. *Biochemistry.* 25:7511–7517.